Singular perturbation with Limit points in the fast dynamics

Matthias Stiefenhofer *†‡

Abstract

A singular perturbation problem in ordinary differential equations is investigated without assuming hyperbolicity of the associated slow manifold. More precisely, the slow manifold consists of a branch of stationary points or a branch of periodic orbits which lose their hyperbolicity at a limit point. Thus, in a neighbourhood of this point a reduction to the slow manifold is not possible. This situation is examined within a generic one parameter unfolding leading in case of a stationary or periodic limit point to a curve of Hopf or Naimark-Sacker bifurcation points with associated periodic orbits or invariant tori respectively. The stationary case is examined in detail with the aim of characterizing the domain in parameter space yielding periodic orbits as precisely as possible. Moreover, the shape and stability of the periodic orbits is determined. The paper examines one case of a not finite determined Bogdanov point with properties partly motivated by formal results in [3].

1 Introduction

In general, an artificial system of the form

$$\dot{x} = f(x,y) \in \mathbb{R}^n, \quad y \in \mathbb{R} \tag{1.1}$$

is used for describing the dynamical behaviour of a natural system for different, but fixed values of the external influence y. In particular, a mathematical model of this kind does not take into consideration the slow variation of y which always exists within the natural system. As a consequence, during large time intervals this simplification typically causes the total deviation of the natural behaviour from the behaviour of the artificial system (1.1). That means, for large time intervals an artificial model of the natural system is forced to take up the dynamics of the previous parameter y. For example this is guaranteed by an extended system of the form

$$\begin{aligned} \dot{x} &= f(x,y) \in \mathbb{R}^n \\ \dot{y} &= \epsilon \cdot g(x,y) \in \mathbb{R}, \quad 0 \leq |\epsilon| \ll 1. \end{aligned} \tag{1.2}$$

*Universität Bielefeld, Fakultät für Mathematik, Postfach 100131, 33501 Bielefeld, Germany

†current address: Universität Tübingen, Lehrstuhl für Biomathematik, Auf der Morgenstelle 10, 72076 Tübingen, Germany

‡supported by DFG Schwerpunktprogramm "Ergodentheorie, Analysis und effiziente Simulation dynamischer Systeme".

Thus, the transition from system (1.1) to system (1.2) is one possibility for dynamically embedding the x-system into a superior (x, y)-system which of course depends itself from external z-influences and the above process of embedding has to be accomplished anew.

From a mathematical point of view, the full (x, y)-system (1.2) represents an ordinary singular perturbation problem, whose features can be investigated with the well known singular perturbation methodes of Fenichel [7] and Vasil'eva [13], but only as long as the assumed y-dependent branch of stationary points $f(x, y) = \Theta \in \mathbb{R}^n$ does not contain a nonhyperbolic point. On the other hand, exactly this loss of validity of the standard theory near a nonhyperbolic point offers the possibility of new and more complex phenomena to arise through the coupling of the fast x-dynamics and the slow y-dynamics. An example of this kind is the formation of invariant tori out of a Hopf point of the fast x-dynamics $\dot{x} = f(x, y)$ [9], [12].

Now in this paper, the case is considered, where the y-dependent branch of the system (1.2) either is a branch of stationary points or a branch of periodic orbits which lose their hyperbolicity at a limit point. More precisely, it is assumed that the fast x-system $\dot{x} = f(x, y)$ possesses a unique branch of stationary points or periodic orbits which contains a stationary point or periodic orbit with simple eigenvalue 0 or double Floquet multiplier 1 respectively.

The case of a stationary quadratic limit point was examined in many papers with special interest in the formation of global relaxation orbits over the intermediate stage of duck orbits [2], [5], [6]. Further, the underlying local formation of periodic orbits out of Hopf points and the subsequent transition to duck orbits is described formally in [3], [4] with the help of asymptotic methods. The sense of the paper in hand now mainly consists of proving analytically some results from [3]. Moreover, the first steps for transfering the results from stationary limit points to limit points of periodic orbits are accomplished. But it should be remarked that with the help of the used scaling technique neither the duck orbits in the stationary case nor the corresponding duck tori in the periodic case can be described. Therefore, only a local analysis in the vicinity of a stationary or periodic limit point is performed.

2 Stationary limit points

The formation of periodic orbits from a stationary limit point of the x-system (1.1) occurs only within the dynamically extended system (1.2) if the curve $g = 0$ intersects the branch of stationary points in the proximity of the limit point. Thus, the system

$$\begin{aligned} \dot{x} &= f(x, y, \epsilon, \lambda) \in \mathbb{R} \\ \dot{y} &= \epsilon \cdot g(x, y, \epsilon, \lambda) \in \mathbb{R}, \quad \epsilon \in \mathbb{R}, \quad \lambda \in \mathbb{R} \end{aligned} \tag{2.1}$$

is considered where the additional parameter $\lambda \in \mathbb{R}$ controls the passage of the curve $g(x, y, \epsilon, \lambda) = 0$, (ϵ, λ) fixed, through the limit point. For the sake of simplicity, the functions f and g are assumed to be of class C^∞. This is also true for all other functions in this paper so that the degree of differentiability is not stated everywhere. Moreover, the relations

$$(f, g)^0 := (f, g)(\Theta) = \Theta, \qquad f_x^0 = 0, \tag{2.2}$$

$$-\, g_x^0 \cdot f_y^0 \neq 0, \qquad f_{xx}^0 \cdot (f_y g_\lambda - g_y f_\lambda)^0 - g_x^0 \cdot (f_{\lambda x} f_y - f_{yx} f_\lambda)^0 \neq 0 \tag{2.3}$$

are assumed where $f_x^0 = 0$ and $-g_x^0 f_y^0 \neq 0$ ensure the transversal intersection of the curves $f(x,y,0,0) = 0$ and $g(x,y,0,0) = 0$ in the origin. The right inequality in (2.3) guarantees that the curve $g = 0$ passes through the limit point with nonvanishing velocity with respect to λ. Hence, under the assumptions (2.2) and (2.3), the following constellations may arise in (x,y)-space for $(\epsilon,\lambda) = \Theta$, with the arrows indicating the trivial phase curves which appear for $\epsilon = 0$ in the direction of the x-axis.

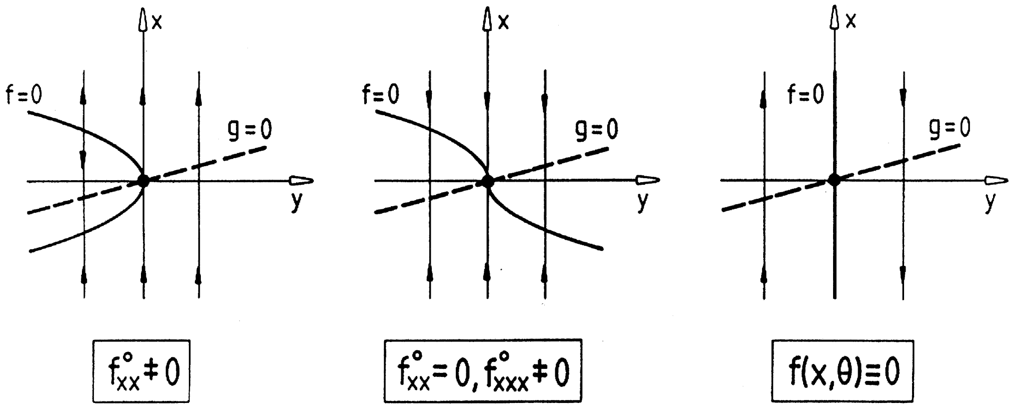

Figure 1: Possible constellations in (x,y)-space for $(\epsilon,\lambda) = \Theta$.

For $\epsilon = 0$ and $\epsilon \neq 0$ the stationary points of the system (2.1) are exactly determined by the solutions of $f(x,y,0,\lambda) = 0 \in \mathbb{R}$ and $(f,g)(x,y,\epsilon,\lambda) = \Theta \in \mathbb{R}^2$ respectively. Thus, according to $f_x^0 = 0$ and $-g_x^0 f_y^0 \neq 0$, the solutions $(x,y,\lambda) = \Theta \in \mathbb{R}^3$ and $(x,y,\epsilon,\lambda) = \Theta \in \mathbb{R}^4$ of the first and second equation can be uniquely continued. This leads to the transversal intersection of the two surfaces

$$(x,y,\epsilon,\lambda) = (x,\bar{y}(x,\lambda),0,\lambda) \quad \text{and} \quad (x,y,\epsilon,\lambda) = (x^s(\epsilon,\lambda),y^s(\epsilon,\lambda),\epsilon,\lambda) \tag{2.4}$$

along the curve of bifurcation points

$$(x,y,\epsilon,\lambda) = (x^s(0,\lambda),y^s(0,\lambda),0,\lambda) \tag{2.5}$$

at $\epsilon = 0$. Furthermore, by (2.2), the linearization of the system (2.1) in the central point $(x,y,\epsilon,\lambda) = \Theta$ possesses the algebraically double and geometrically simple eigenvalue 0 which generally splits under a perturbation within the nontrivial surface $(x,y)^s(\epsilon,\lambda)$ into two eigenvalues different from 0. However, with the help of the two degrees of freedom on this manifold of stationary points, it will be possible to adjust the two eigenvalues on the imaginary axis implying the existence of a curve of Hopf points.

Now, the formation of a curve of Hopf points out of a stationary point with algebraically double and geometrically simple eigenvalue 0 corresponds exactly to the situation within a two parameter unfolding of a finite determined Bogdanov point [8]. However, these Bogdanov points additionally cause a curve of homoclinic orbits representing the border of the periodic orbits which branch off from the curve of Hopf points. On contrary, in case of the not finite determined singular perturbation problem (2.1), no homoclinic orbits can arise from the central point $(x,y,\epsilon,\lambda) = \Theta$, because only one stationary point survives from the branch of stationary points when passing from $\epsilon = 0$ to $\epsilon \neq 0$. Hence, the region of existence of the periodic orbits seems not clear. Yet, the analysis in [2], [3], [4], [5], [6] shows that instead of homoclinic orbits, an exponentially narrow strip of duck orbits has to be expected. These duck orbits are typically representing an intermediate stage to some global object such as relaxation orbits or homoclinic orbits [10]. Now, in the following theorem, it is tried to describe the domain in the (ϵ, λ)-parameter space between the curve of Hopf points and the strip of duck orbits as precisely as possible. Furthermore, the shape and stability of the periodic orbits is determined.

First of all, under the assumption $-g_x^0 f_y^0 > 0$ (compare (2.3)), the subsequent constants are well defined by derivatives of f and g in the central point $(x, y, \epsilon, \lambda) = \Theta$:

$$\begin{aligned} d &:= (-g_x^0 f_y^0)^{\frac{1}{2}} > 0, \\ A &:= \tfrac{1}{d^3}\cdot (f_{xx}(f_y g_\epsilon - g_y f_\epsilon) - g_x(f_{\epsilon x} f_y - f_{yx} f_\epsilon))^0, \\ B &:= \tfrac{1}{d^3}\cdot (f_{xx}(f_y g_\lambda - g_y f_\lambda) - g_x(f_{\lambda x} f_y - f_{yx} f_\lambda))^0 \neq 0 \quad \text{(cf. (2.3))}, \\ C &:= f_{xy}^0, \\ D &:= \tfrac{1}{6d}\cdot (f_{xxx} f_y^2 - 3 f_{xy} f_{xx} f_y)^0, \\ E &:= \tfrac{1}{d}\cdot (f_{xx} f_y)^0, \\ F &:= \tfrac{1}{2d^2}\cdot (g_{xx} f_y^2 - g_y f_{xx} f_y)^0, \\ G &:= \tfrac{1}{d}\cdot g_y^0, \\ R &:= -\tfrac{1}{3B}\cdot ((C+F)E + 3D) \ . \end{aligned} \tag{2.6}$$

Then the following results are valid for the system (2.1) under the assumptions (2.2), (2.3) and $-g_x^0 f_y^0 > 0$.

Theorem 2.1:

i. The central point $(x, y, \epsilon, \lambda) = \Theta$ represents an end point of a curve of Hopf points $(x, y, \epsilon, \lambda) = (x_h(\epsilon), y_h(\epsilon), \epsilon, \lambda_h(\epsilon))$, $0 < \epsilon < \delta(0) \ll 1$ with $\lambda_h'(\epsilon) \to -(A+G)/B$ for $\epsilon \to 0$ and associated eigenvalues of order $\pm i\cdot O(\sqrt{\epsilon})$ for $\epsilon \to 0$.

ii. In $(u, \bar{\epsilon})$-space there exists an open neighbourhood V of the u-axis, a function $\tau(u, \bar{\epsilon}) \in \mathbb{R}$ defined in V with $\tau(0, \bar{\epsilon}) = 0$, and an u-dependent family of curves $\lambda_u(\epsilon) := \lambda_h(\epsilon) + \epsilon\cdot \tau(u, \sqrt{\epsilon})$, $0 < \epsilon < \delta(u) \ll 1$ in parameter space, so that for fixed $u > 0$ a branch of periodic orbits arises from the central point $(x, y) = \Theta$ along the curve $(\epsilon, \lambda) = (\epsilon, \lambda_u(\epsilon))$. The periodic orbits converge in x- and y-direction with order $O(\sqrt{\epsilon})$ and $O(\epsilon)$ to this point, whereas the period of the orbits tends to ∞ with order $1/O(\sqrt{\epsilon})$.

iii. The function $\tau(u, 0)$, $u \in \mathbb{R}$ satisfies

$$\tau(u, 0) = \tfrac{3}{4} R u^2 \cdot (1 + O(Eu)),$$

$$\tau(u, 0) = \tau(-u, 0) \quad \text{and} \quad \tau(u, 0) > (<)\ 0 \quad \text{for} \quad R > (<)\ 0, \quad u \neq 0 \ .$$

iv. The periodic orbits along $\lambda_u(\epsilon)$ *from ii are stable (unstable) if*

$$R\cdot B > (<)\ 0 \qquad \textit{and} \qquad \begin{cases} 0 < u \ll 1, & \textit{in case of} \quad E \neq 0 \\ 0 < u < \infty, & \textit{in case of} \quad E = 0\ . \end{cases}$$

Now by i, a one-sided curve of Hopf points starts out of the central point $(x, y, \epsilon, \lambda) = \Theta$ for $\epsilon > 0$ and $\lambda = \lambda_h(\epsilon)$. Then, because of $\tau(0, \sqrt{\epsilon}) = 0$ and $\lambda_u(\epsilon) = \lambda_h(\epsilon) + \epsilon\cdot\tau(u, \sqrt{\epsilon})$ (compare ii), this curve of Hopf points passes over for fixed $u > 0$ into a curve of periodic orbits parametrized by ϵ. Further a Taylor expansion with respect to $\bar{\epsilon}$ of the function $\tau(u, \bar{\epsilon})$ yields

$$\lambda_u(\epsilon) = \lambda_h(\epsilon) + \epsilon\cdot\tau(u, 0) + \epsilon^{\frac{3}{2}}\cdot\tau_{\bar{\epsilon}}(u, 0) + O(\epsilon^2), \tag{2.7}$$

and consequently the slope of this curve in the central point reads

$$\lambda'_u(0) = \lambda'_h(0) + \tau(u, 0). \tag{2.8}$$

Thus, iii and $R > 0$ imply $\lambda'_u(0) > \lambda'_h(0)$, and together with the additional assumptions $\lambda'_h(0) = -(A + G)/B > 0$ and $B > 0$, one obtains the following bifurcation diagram of periodic orbits ($= Po$) along the parameter curves $(\epsilon, \lambda) = (\epsilon, \lambda_u(\epsilon))$, $0 < \epsilon < \delta(u)$, $0 < u \ll 1$ (cf. i, ii, iv).

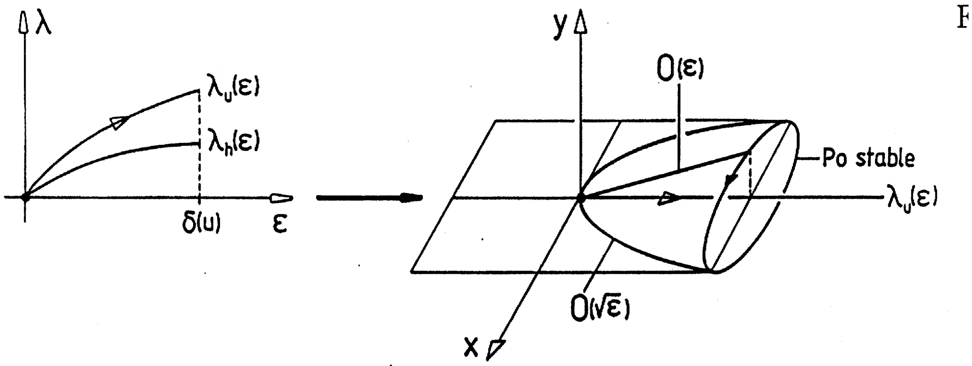

Figure 2: Bifurcation diagram along the curve $\lambda_u(\epsilon)$.

Now, the range of $\tau(u, 0)$, $u \in \mathbb{R}$ (cf. (2.8)) determines the possible slopes within the family $\lambda_u(\epsilon)$ at $\epsilon = 0$. Moreover, by iii, these curves are locally situated for $R > 0$ or $R < 0$ completely above or below the curve of Hopf points $\lambda_h(\epsilon)$. Further, a simple calculation shows that the periodic orbits arise through the transition of a saddle ($\epsilon < 0$) into a source or a sink ($\epsilon > 0$). This corresponds again to the situation within a two parameter unfolding of a finite determined Bogdanov point along parameter curves between the curve of Hopf points and the curve of homoclinic orbits.

In case of $R \neq 0$, $E = 0$, the range of $\tau(u, 0) = \frac{3}{4}\cdot Ru^2$ (compare iii) agrees with $(0, \infty)$ or $(-\infty, 0)$ for $R > 0$ or $R < 0$ respectively, so that the functions $\lambda_u(\epsilon)$ pass the complete region from the curve of Hopf points $\lambda_h(\epsilon)$ up to the positive or negative λ-axis. However, it should be noted, that the domain of definition $0 < \epsilon < \delta(u)$ of $\lambda_u(\epsilon)$ might become arbitrarily small if u tends towards $\pm\infty$. On contrary, in case of $R = 0$ one obtains from iii and (2.7) the identities $\tau(u, 0) = 0$ and $\lambda_u(\epsilon) = \lambda_h(\epsilon) + \epsilon^{\frac{3}{2}}\cdot\tau_{\bar{\epsilon}}(u, 0) + O(\epsilon^2)$, so that all the curves $\lambda_u(\epsilon)$

are tangentially touching the curve of Hopf points $\lambda_h(\epsilon)$ at $\epsilon = 0$. Of course, the equalities $\tau(u, \sqrt{\epsilon}) \equiv 0$ and $\lambda_u(\epsilon) \equiv \lambda_h(\epsilon)$ are also possible which occur exemplarily in case of the simple integral system $\dot{x} = y - x^2, \ \dot{y} = \epsilon \cdot (\lambda - x)$.

Now, the previous cases $R \neq 0, \ E = 0$ and $R = 0$ are only covering degenerate situations, while unfortunately the generic case $R \neq 0, \ E \neq 0$ can not be discussed completely. However, it can be shown that in this situation a symmetric function $S(\bar{u}) : \mathbb{R} \to \mathbb{R}$ exists with $S(0) = 0$ and $\tau(u, 0) = R \cdot S(Eu)/E^2$, so that the range of $\tau(u, 0)$ is determined by the range of $S(\bar{u})$. Numerical calculations (compare section 5) and approximations in [3] are now indicating that $S(\bar{u})$ converges strictly monotone towards 3 as $\bar{u}$ tends to $\pm\infty$, and therefore $\tau(u, 0)$ presumably converges strictly monotone to $3R/E^2$. With this limiting behaviour and with the associated notation $\hat{\lambda}(\epsilon) := \lambda_h(\epsilon) + \epsilon \cdot 3R/E^2$, one obtains the following qualitative diagrams in the (ϵ, λ)-parameter space for $R \geq 0$ and $\lambda'_h(0) = -(A + G)/B > 0$.

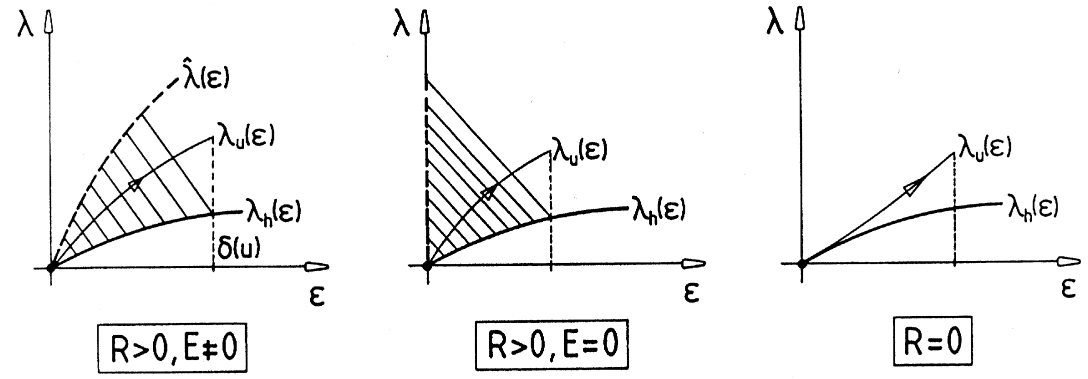

Figure 3: Domaines of existence of the periodic orbits.

Note that the middle case in Fig.3 is excluded for a quadratic limit point of the x-system (compare left diagram in Fig.1), because of $f^0_{xx} \neq 0$ and $E = f^0_{xx} f^0_y / d \neq 0$, whereas this case always occurs for a cusp point, that is for $f^0_{xx} = 0, \ f^0_{xxx} \neq 0$ (compare middle diagram in Fig.1). Moreover, in case of $f^0_{xx} = f^0_{xxx} = 0$ (compare right diagram in Fig.1), it follows $R = 0$ yielding the right diagram in Fig.3. Further, in the left and middle diagram of Fig.3, the curves $\lambda_u(\epsilon)$ are locally situated for $0 < \epsilon < \delta(u) \ll 1$ within the hatched region proposing that the duck orbits appear in case of $R > 0, \ E \neq 0$ just on curves in the direction of the sector border $\hat{\lambda}(\epsilon) = \lambda_h(\epsilon) + \epsilon \cdot 3R/E^2$. At least, this is true concerning the duck orbits investigated in [6]. Finally, in case of a cusp point $R > 0, \ E = 0$, the duck orbits can arise at most on parameter curves which are tangentially touching the λ-axis, whereas in case of $R = 0$ a prediction with respect to these orbits seems rather difficult.

Summing up all previous results for the generic case $R \neq 0, \ E \neq 0$, the system (2.1) typically causes a (ϵ, λ, x)-bifurcation diagram shown in Fig.4 below.

Thus, there exists a curve of bifurcation points BP_s (compare (2.5)) which represents the intersection of a continuum of stationary points SC at $\epsilon = 0$ and a surface of stationary points SP which arises for $\epsilon \neq 0$. Moreover, the surface SP contains a one-sided curve of Hopf points $\lambda_h(\epsilon)$ leading to periodic orbits Po. However, the limiting behaviour of these orbits as λ tends to the border $\hat{\lambda}(\epsilon)$ of the hatched sector is drawn arbitrarily. In this region duck orbits appear.

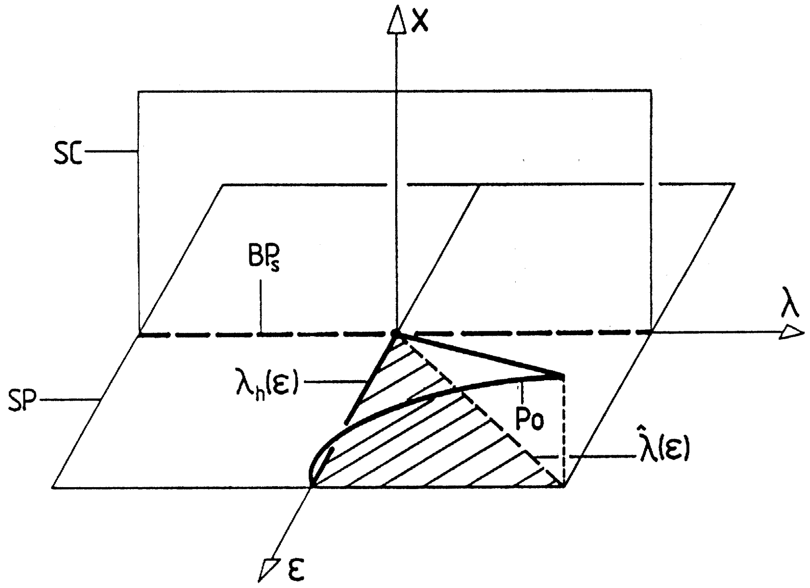

Figure 4: (ϵ, λ, x)–bifurcation diagram for $R \neq 0$, $E \neq 0$. SP = stationary point, SC =stationary continuum, BP_s = bifurcation point, Po = periodic orbit.

Further, note that the stability result iv in Theorem 2.1 only extends the well known principle of exchange of stability between stationary and periodic branch at a Hopf point to the case of a stationary point with double eigenvalue 0. Strictly speaking, the signs of R and B determine the bifurcation direction of the periodic orbits in the direction of λ and the direction of the complex–conjugate pair of eigenvalues which cross the imaginary axis at the Hopf points $\lambda = \lambda_h(\epsilon)$.

Finally, in case of $-g_x^0 f_y^0 < 0$, the trivial transformation $\epsilon \to -\epsilon$ yields a system which can be investigated with Theorem 2.1. Moreover, all results of this section can be extended to systems of the form $\dot{x} = F(x, y, \epsilon, \lambda) \in \mathbb{R}^n$, $\dot{y} = \epsilon \cdot g(x, y, \epsilon, \lambda) \in \mathbb{R}$ with the help of a reduction to an appropriate center manifold [12]. The proof of Theorem 2.1 appears in a rather extensive form in [12] and in a shorter form in the sections 4 and 5 of this paper. Furthermore, in [12] a general scheme concerning singular perturbed non–hyperbolic points is developed and partly investigated with the help of analytical and numerical methods.

3 Periodic limit points

In this section a 3-dimensional system of the singular perturbation form

$$\begin{aligned} \dot{x} &= f(x, y, \epsilon, \lambda) \in \mathbb{R}^2 \\ \dot{y} &= \epsilon \cdot g(x, y, \epsilon, \lambda) \in \mathbb{R} \end{aligned} \tag{3.1}$$

is considered with flow $(\Psi, \varphi)(t, x_1, x_2, y, \epsilon, \lambda) \in \mathbb{R}^2 \times \mathbb{R}$ and T-periodic solution $(\Psi, \varphi)(t, \Theta)$. Then, this T-periodic solution at the parameter value $(\epsilon, \lambda) = \Theta$ represents a T-periodic solution of the pure x-system $\dot{x} = f(x, \Theta)$ which satisfies $\dot{\Psi}_2(T, \Theta) \neq 0$ without loss of generality. Thus, a locally unique function $t(x_1, y, \epsilon, \lambda)$ of class C^∞ exists with $t(\Theta) = T$ and

$\Psi_2(t(x_1,y,\epsilon,\lambda),x_1,0,y,\epsilon,\lambda)=0$. Consequently, the flow (Ψ,φ) causes a discrete dynamics in the (x_1,y)-plane for (x_1,y,ϵ,λ) near Θ which is determined by the Poincaré-iteration

$$\begin{aligned}
x_1^{n+1} &= x_1^n + \Psi_1(t(x_1^n,y^n,\epsilon,\lambda),x_1^n,0,y^n,\epsilon,\lambda) - x_1^n \\
&=: x_1^n + F(x_1^n,y^n,\epsilon,\lambda) \in \mathbb{R} \\
y^{n+1} &= y^n + \varphi(t(x_1^n,y^n,\epsilon,\lambda),x_1^n,0,y^n,\epsilon,\lambda) - y^n \\
&= y^n + \epsilon\cdot\{\varphi_\epsilon(t(x_1^n,y^n,0,\lambda),x_1^n,0,y^n,0,\lambda)+O(\epsilon)\} \\
&= y^n + \epsilon\cdot\{\int_0^{t(x_1^n,y^n,0,\lambda)} g(\Psi(s,x_1^n,0,y^n,0,\lambda),y^n,0,\lambda)\ ds + O(\epsilon)\} \\
&=: y^n + \epsilon\cdot G(x_1^n,y^n,\epsilon,\lambda) \in \mathbb{R}\ .
\end{aligned} \tag{3.2}$$

Note that $\varphi(t,x,y,0,\lambda)=y$ and

$$\dot{\varphi}_\epsilon(t,x,y,0,\lambda)=g(\Psi(t,x,y,0,\lambda),y,0,\lambda), \quad \varphi_\epsilon(0,x,y,0,\lambda)=\Theta\ .$$

Hence the continuous 3-dimensional singular perturbation problem (3.1) transfers straightforward into this discrete singular perturbed system in the plane allowing now the adoption of the stationary assumptions (2.2) and (2.3) for periodic orbits. For this purpose, one only has to replace (f,g) by (F,G) and x by x_1 leading to

$$(F,G)^0 := (F,G)(\Theta)=\Theta, \qquad F^0_{x_1}=0, \tag{3.3}$$

$$-G^0_{x_1}\cdot F^0_y \neq 0, \qquad F^0_{x_1x_1}\cdot(F_yG_\lambda - G_yF_\lambda)^0 - G^0_{x_1}\cdot(F_{x_1\lambda}F_y - F_{x_1y}F_\lambda)^0 \neq 0\ . \tag{3.4}$$

These assumptions ensure again the transversal intersection of the curves $F(x_1,y,0,0)=0$ and $G(x_1,y,0,0)=0$ in the central point $(x_1,y)=\Theta$ resulting graphically in Fig.1 with the corresponding modifications. On the other hand, from a dynamical point of view, the curve $F(x_1,y,0,0)=0$ marks the y-dependent branch of periodic orbits of the fast x-system $\dot{x}=f(x,y,0,0)\in\mathbb{R}^2$ (compare (3.1)), whereas the curve $G(x_1,y,0,0)=0$ characterizes the solutions which consider a certain averaging condition. Therefore, in contrast to the curve $g=0$ in the stationary case, the curve $G=0$ can not be interpreted in a direct way. Furthermore, the existence of two manifolds of periodic orbits (compare (2.4)) which intersect transversally along a curve of bifurcation points (compare (2.5)) results again from (3.3), (3.4). Apart from this first correspondence between stationary and periodic limit points, now in the following it will be shown that the Poincaré-iteration (3.2) possesses also a one-sided curve of Hopf points (cf. Theorem 2.1 i). Generically these Hopf points imply the existence of closed invariant curves of the Poincaré-iteration.

More precisely, the linearization of the Poincaré-map assumes the form

$$A(x_1,y,\epsilon,\lambda) := \begin{pmatrix} 1+F_{x_1} & F_y \\ \epsilon\cdot G_{x_1} & 1+\epsilon\cdot G_y \end{pmatrix} (x_1,y,\epsilon,\lambda) \tag{3.5}$$

with eigenvalues $\frac{1}{2}\cdot \operatorname{tr} A(x_1,y,\epsilon,\lambda) \pm \frac{i}{2}\cdot\sqrt{4\cdot \det A(x_1,y,\epsilon,\lambda) - \operatorname{tr}^2 A(x_1,y,\epsilon,\lambda)}$ and tr (det) denoting the trace (determinant) of the corresponding matrix. Therefore, the Hopf points of the Poincaré-iteration, i.e. the fixed points with an unreal pair of complex-conjugate eigenvalues on the unit circle, are exactly given by the solutions of

$$H(x_1,y,\epsilon,\lambda) := \begin{pmatrix} F(x_1,y,\epsilon,\lambda) \\ G(x_1,y,\epsilon,\lambda) \\ \det A(x_1,y,\epsilon,\lambda) - 1 \end{pmatrix} = \Theta, \qquad H : \mathbb{R}^4 \to \mathbb{R}^3$$

which satisfy $4 - \mathrm{tr}^2 A(x_1,y,\epsilon,\lambda) > 0$. Now, the central point $(x_1,y,\epsilon,\lambda) = \Theta$ obviously is a solution of this equation where $A(\Theta)$ possesses the algebraically double and geometrically simple eigenvalue 1 (compare (3.3)-(3.5)), yet with $4 - \mathrm{tr}^2 A(\Theta) = 0$. Moreover, a simple calculation together with the non-degeneracy condition (3.4) shows the regularity of $H_{x_1,y,\lambda}(\Theta) \in \mathbb{R}^{3,3}$ yielding a locally unique function $(x_1,y,\lambda)_h(\epsilon)$ with $(x_1,y,\lambda)_h(0) = \Theta$ and $H(x_{1h}(\epsilon), y_h(\epsilon), \epsilon, \lambda_h(\epsilon)) = \Theta$. Thus, with the abbreviation $D(\epsilon) := 4 - \mathrm{tr}^2 A(x_{1h}(\epsilon), y_h(\epsilon), \epsilon, \lambda_h(\epsilon))$, the identity $D(0) = 0$ results. Further a direct calculation shows $D'(0) \neq 0$ implying in case of $D'(0) > (<)\ 0$ the bifurcation of a one-sided curve of Hopf points $(x_{1h}(\epsilon), y_h(\epsilon), \epsilon, \lambda_h(\epsilon))$ out of the central point $(x_1,y,\epsilon,\lambda) = \Theta$ for $\epsilon > (<)\ 0$.

From these Hopf points closed invariant curves of the Poincaré-iteration with radius $O(\sqrt{\lambda})$ branch off in λ-direction by a Naimark-Sacker bifurcation if the pair of complex-conjugate eigenvalues passes the unit circle with non-vanishing velocity and if additionally an internal non-degeneracy condition is satisfied [8]. Now, the external parameter condition of velocity follows after a simple calculation again from (3.4), whereas the internal condition depends on higher derivatives of F and G which were not examined in detail. But in principle, a constant corresponding to R (compare (2.6)) must be calculated. This constant determines the bifurcation direction of the invariant curves along the λ-axis.

Thus, from a dynamical point of view, a degenerate branch of periodic orbits with a pair of complex-conjugate Floquet multipliers on the unit circle arises from the point $(x,y,\epsilon,\lambda) = \Theta$. Generically this yields a 2-dimensional manifold of invariant tori. Altogether, one obtains a bifurcation diagram analogous to Fig.4 if the surfaces of stationary points SP and SC as well as the periodic orbits Po are replaced by periodic orbits and invariant tori respectively. However, the demonstrated basic results of this section obviously do not yield a border line $\hat{\lambda}(\epsilon)$, so that the domain of existence of the invariant tori remains completely unknown as ϵ tends to 0. Furthermore, the question remains open, to what extend the transfer of the other statements ii-iv from Theorem 2.1 as well as the transfer of the indicated duck properties to duck tori is possible?

4 Scaling and back substitution

In this section the 2-dimensional system (2.1) is considered under the assumptions (2.2), (2.3) and with the abbreviations (2.6). Now, the direct examination of this system along parameter curves of the form $\lambda_u(\epsilon)$ (compare Fig.2 and Fig.3) does not seem very promising, because for $\epsilon = 0$ a system with 1-dimensional dynamics appears (compare Fig.1) which prevents the construction of an appropriate Poincaré-map for proving the existence of periodic orbits. Thus, the $\epsilon = 0$ system must be replaced by another system. For this purpose, the coordinates (x,y) are stretched in dependence of ϵ along $\lambda_u(\epsilon)$ in such a way that in the new coordinates $(\bar{x},\bar{y})$ a possibly existing branch of periodic orbits does not shrink to a stationary point, but remains a periodic orbit as ϵ tends to 0. Then, starting from this artificially constructed orbit at $\epsilon = 0$ it reversely might be possible to establish the branch of periodic orbits for $\epsilon \neq 0$.

More precisely, in the first step the stationary points $(x,y)^s(\epsilon,\lambda)$ from equation (2.4) are shifted to the origin of phase space as usual. Subsequently the semi space $\{(x,y,\epsilon,\lambda)|\epsilon > 0\}$ is mapped according to the two transformations

$$(\bar{x},\bar{y},\bar{\epsilon},\bar{\lambda}) \;=\; \left(\frac{x}{f_y^0\sqrt{\epsilon}}\;,\;\frac{y}{d\epsilon}+\frac{f_{xx}^0x^2}{2df_y^0\epsilon}\;,\;\sqrt{\epsilon}\;,\;\frac{\lambda}{\epsilon}+\frac{A+G}{B}\right) \;=:\; T_+(x,y,\epsilon,\lambda)$$

and

$$(\bar{x},\bar{y},\bar{\epsilon},\bar{\lambda}) \;=\; \left(-\frac{x}{f_y^0\sqrt{\epsilon}}\;,\;\frac{y}{d\epsilon}+\frac{f_{xx}^0x^2}{2df_y^0\epsilon}\;,\;-\sqrt{\epsilon}\;,\;\frac{\lambda}{\epsilon}+\frac{A+G}{B}\right) \;=:\; T_-(x,y,\epsilon,\lambda)$$

into the two semi spaces $\{(\bar{x},\bar{y},\bar{\epsilon},\bar{\lambda})|\bar{\epsilon} > 0\}$ and $\{(\bar{x},\bar{y},\bar{\epsilon},\bar{\lambda})|\bar{\epsilon} < 0\}$ with inverse mappings

$$(x,y,\epsilon,\lambda) \;=\; \left(f_y^0\bar{\epsilon}\bar{x}\;,\;\bar{\epsilon}^2\cdot(d\bar{y}-\tfrac{1}{2}f_{xx}^0f_y^0\bar{x}^2)\;,\;\bar{\epsilon}^2\;,\;\bar{\epsilon}^2\cdot(\bar{\lambda}-\frac{A+G}{B})\right) \;=:\; T_\pm^{-1}(\bar{x},\bar{y},\bar{\epsilon},\bar{\lambda})$$

(compare also [3]). In particular, the two inverse mappings T_+^{-1} and T_-^{-1} obviously can be connected to a mapping of class C^∞ along $\{(\bar{x},\bar{y},\bar{\epsilon},\bar{\lambda})|\bar{\epsilon} = 0\}$. This property holds also true for the two transformed systems resulting in the connected system

$$\begin{aligned}
\dot{\bar{x}} &= d\bar{\epsilon}\cdot\{\bar{y}+\bar{\epsilon}\cdot[(B\bar{\lambda}-G)\bar{x}+C\bar{x}\bar{y}+D\bar{x}^3]+\bar{\epsilon}^2\cdot r_1(\bar{x},\bar{y},\bar{\epsilon},\bar{\lambda})\}\\
&=: d\bar{\epsilon}\cdot\bar{f}(\bar{x},\bar{y},\bar{\epsilon},\bar{\lambda})\\
\dot{\bar{y}} &= d\bar{\epsilon}\cdot\{(E\bar{y}-1)\bar{x}+\bar{\epsilon}\cdot[\;E\bar{x}\cdot[(B\bar{\lambda}-G)\bar{x}+C\bar{x}\bar{y}+D\bar{x}^3]+G\bar{y}+F\bar{x}^2\;]\\
&\quad+\bar{\epsilon}^2\cdot r_2(\bar{x},\bar{y},\bar{\epsilon},\bar{\lambda})\}\\
&=: d\bar{\epsilon}\cdot\bar{g}(\bar{x},\bar{y},\bar{\epsilon},\bar{\lambda})
\end{aligned} \tag{4.1}$$

with functions $r_1, r_2, \bar{f}, \bar{g}$ of class C^∞ which are defined in an open neighbourhood of $\{(\bar{x},\bar{y},\bar{\epsilon},\bar{\lambda})|\bar{\epsilon} = 0\}$. Note that according to the transformations T_+ and T_-, the solution of the system (4.1) with parameter value $(-\bar{\epsilon},\bar{\lambda}), \bar{\epsilon} \neq 0$ and initial value $(-\bar{x},\bar{y})$ arises from the solution of this system with parameter value $(\bar{\epsilon},\bar{\lambda})$ and initial value $(\bar{x},\bar{y})$ by reflection at the $\bar{y}$-axis. Therefore, the system (4.1) shows the same phenomena for $\bar{\epsilon} > 0$ and $\bar{\epsilon} < 0$. Further, after the scaling of time

$$t = \frac{s}{d\bar{\epsilon}}\;, \tag{4.2}$$

the equation (4.1) obviously transforms to $\dot{\bar{x}} = \bar{f}(\bar{x},\bar{y},\bar{\epsilon},\bar{\lambda})$, $\dot{\bar{y}} = \bar{g}(\bar{x},\bar{y},\bar{\epsilon},\bar{\lambda})$ with unique stationary points $(\bar{x},\bar{y},\bar{\epsilon},\bar{\lambda}) = (0,0,\bar{\epsilon},\bar{\lambda})$ and associated eigenvalues $\sigma(\bar{\epsilon},\bar{\lambda})\pm i\cdot\omega(\bar{\epsilon},\bar{\lambda})$, $(\sigma,\omega)(\bar{\epsilon},\bar{\lambda}) \in \mathbb{R}^2$ with

$$\begin{aligned}
&\sigma(0,\bar{\lambda}) = 0, && \omega(0,\bar{\lambda}) = 1,\\
&\sigma(\bar{\epsilon},\bar{\lambda}) = -\sigma(-\bar{\epsilon},\bar{\lambda}) \quad \text{and} && \omega(\bar{\epsilon},\bar{\lambda}) = \omega(-\bar{\epsilon},\bar{\lambda})
\end{aligned} \tag{4.3}$$

(compare T_+, T_- and $t = \dfrac{s}{d\bar{\epsilon}}$). Then, with the additional transformations

$$\begin{aligned}
\begin{pmatrix} \bar{x} \\ \bar{y} \end{pmatrix} &= \frac{1}{\omega(\bar{\epsilon},\bar{\lambda})} \begin{pmatrix} \omega(\bar{\epsilon},\bar{\lambda}) & \frac{1}{2}(\bar{g}_{\bar{y}} - \bar{f}_{\bar{x}})(\Theta,\bar{\epsilon},\bar{\lambda}) \\ 0 & -\bar{g}_{\bar{x}}(\Theta,\bar{\epsilon},\bar{\lambda}) \end{pmatrix} \cdot \begin{pmatrix} u \\ v \end{pmatrix} =: (\rho,\gamma)(\bar{\epsilon},\bar{\lambda}) \cdot \begin{pmatrix} u \\ v \end{pmatrix}, \\
s &= \frac{\bar{t}}{\omega(\bar{\epsilon},\bar{\lambda})}
\end{aligned} \tag{4.4}$$

where the vectors $\rho(\bar{\epsilon},\bar{\lambda}),\ \gamma(\bar{\epsilon},\bar{\lambda}) \in \mathbb{R}^2$ denote the real- and imaginary part of an eigenvector to the eigenvalue $\sigma(\bar{\epsilon},\bar{\lambda}) + i\cdot\omega(\bar{\epsilon},\bar{\lambda})$, the final system $(\dot{u},\dot{v}) =: \dot{w} = H(w,\bar{\epsilon},\bar{\lambda}) \in \mathbb{R}^2$ results which satisfies

$$\begin{aligned}
& H(w,\bar{\epsilon},\bar{\lambda}) = \Theta && \Leftrightarrow && (w,\bar{\epsilon},\bar{\lambda}) = (\Theta,\bar{\epsilon},\bar{\lambda}), \\
& H_w(\Theta,\bar{\epsilon},\bar{\lambda}) = && \frac{1}{\omega(\bar{\epsilon},\bar{\lambda})} \begin{pmatrix} \sigma & \omega \\ -\omega & \sigma \end{pmatrix} (\bar{\epsilon},\bar{\lambda}) && =: \begin{pmatrix} \bar{\sigma}(\bar{\epsilon},\bar{\lambda}) & 1 \\ -1 & \bar{\sigma}(\bar{\epsilon},\bar{\lambda}) \end{pmatrix}, \\
& \bar{\sigma}(0,\bar{\lambda}) = 0 && \text{and} && \bar{\sigma}(\bar{\epsilon},\bar{\lambda}) = -\bar{\sigma}(-\bar{\epsilon},\bar{\lambda})\ .
\end{aligned} \tag{4.5}$$

In detail, this transformed system assumes the form

$$\begin{aligned}
\dot{u} &= v + \bar{\epsilon}\cdot\{\tfrac{1}{2}B\bar{\lambda}(Ev+1)u + (C-GE)uv + Du^3\} + O(\bar{\epsilon}^2) \\
&= H_1(u,v,\bar{\epsilon},\bar{\lambda}) \\
\dot{v} &= (Ev-1)u \\
&\quad + \bar{\epsilon}\cdot\{\tfrac{1}{2}B\bar{\lambda}v + (BE\bar{\lambda} - GE + F)u^2 - (\tfrac{1}{2}BE\bar{\lambda} - GE)v^2 + CEu^2v + DEu^4\} + O(\bar{\epsilon}^2) \\
&= H_2(u,v,\bar{\epsilon},\bar{\lambda})
\end{aligned} \tag{4.6}$$

defined in an open neighbourhood of $\{(u,v,\bar{\epsilon},\bar{\lambda}) | \bar{\epsilon} = 0\}$ with corresponding flow $\varphi(\bar{t},u,v,\bar{\epsilon},\bar{\lambda})$. Moreover, concerning the complete transformation of the original variables (x,y,ϵ,λ,t), $\epsilon > 0$ of the system (2.1) into the final variables $(u,v,\bar{\epsilon},\bar{\lambda},\bar{t})$, $\bar{\epsilon} > 0$ of the system (4.6), it follows under consideration of T_+^{-1} and (2.4), (4.2)–(4.4)

$$\begin{aligned}
& \epsilon = \bar{\epsilon}^2, \qquad \lambda = \bar{\epsilon}^2\cdot(\bar{\lambda} - (A+G)/B), \qquad t = \frac{\bar{t}}{d\bar{\epsilon}\cdot\omega(\bar{\epsilon},\bar{\lambda})} = \frac{\bar{t}}{O(\bar{\epsilon})}, \\
& x = x^s(\bar{\epsilon}^2, \bar{\epsilon}^2\cdot(\bar{\lambda} - (A+G)/B)) + \bar{\epsilon}\cdot f_y^0 u + O(\bar{\epsilon}^2)v = O(\bar{\epsilon}), \\
& y = y^s(\bar{\epsilon}^2, \bar{\epsilon}^2\cdot(\bar{\lambda} - (A+G)/B)) + \bar{\epsilon}^2\cdot(dv - \tfrac{1}{2}f_{xx}^0 f_y^0 u^2) + O(\bar{\epsilon}^3)v = O(\bar{\epsilon}^2)\ .
\end{aligned} \tag{4.7}$$

Further, according to (4.6), the artificially constructed $\bar{\epsilon} = 0$ system reads

$$\begin{pmatrix} \dot{u} \\ \dot{v} \end{pmatrix} = \begin{pmatrix} v \\ (Ev-1)u \end{pmatrix} = \begin{pmatrix} 0 & 1 \\ -1 & 0 \end{pmatrix} \begin{pmatrix} u \\ v \end{pmatrix} + \begin{pmatrix} 0 \\ Euv \end{pmatrix} \tag{4.8}$$

depending only on the constant $E = f_{xx}^0 f_y^0 / d$ which motivates the notation $\phi(\bar{t},u,v,E) = \varphi(\bar{t},u,v,0,\bar{\lambda})$ for the flow of this system. Now for $E = 0$ and $E \neq 0$ one obtains

$$\phi(\bar{t},u,0,0) = u\cdot(\cos(\bar{t}), -\sin(\bar{t})) \qquad \text{and} \qquad \phi(\bar{t},u,0,E) = \frac{\phi(\bar{t},Eu,0,1)}{E} \tag{4.9}$$

respectively, so that in case of $E \neq 0$, the system (4.8) only has to be investigated for $E = 1$. This $E = 1$ system possesses the integral $I(u,v) = u^2 - 2v - 2\ln(1-v)$, $u \in \mathbb{R}$, $v < 1$ which determines the trajectory of $\phi(\bar{t}, u_0, 0, 1)$ by $u^2 - 2v - 2\ln(1-v) = u_0^2$. Therefore, the trajectories are symmetrically positioned with respect to the v-axis leading to the left diagram in Fig.5 below, whereas the right diagram represents the phase plane of the system (4.8) for $E = 0$.

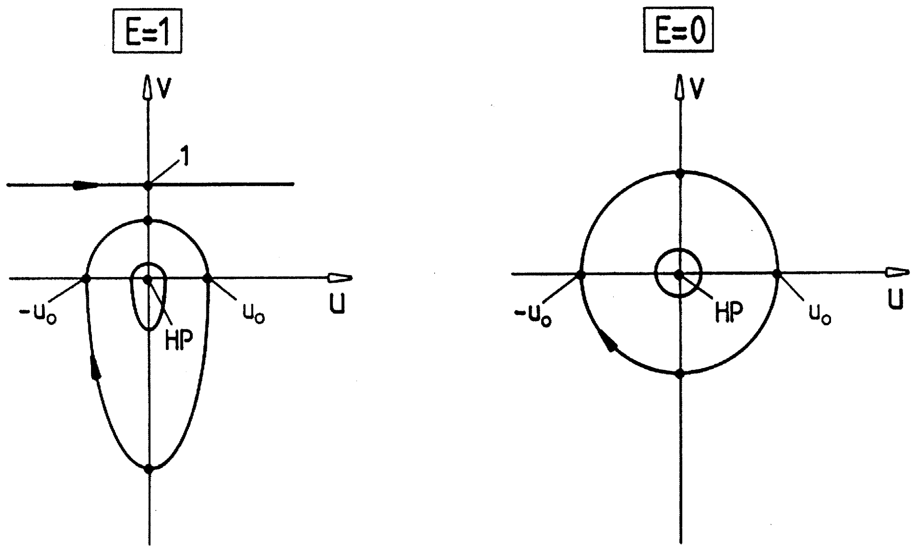

Figure 5: The artificially constructed scaled integral system at $\bar{\epsilon} = 0$. HP = Hopf point.

The period of the solution with initial value $(u,v) = (u_0, 0)$ will be denoted with $T(u_0, E)$. After these preliminary statements concerning the scaled integral system (4.8), now the actually interesting features of the full system (4.6) are comprised in the next theorem.

Theorem 4.1:

i. For $u \neq 0$ the $\bar{\epsilon} = 0$ system (4.8) possesses the $T(u,E)$-periodic solution $\phi(\bar{t}, u, 0, E)$ with

$$\begin{cases} T(0,E) = 2\pi \quad \text{and} \quad T(u,E) \to +\infty \quad \text{for} \quad u \to \pm\infty, \quad if \quad E \neq 0 \\ T(u,0) \equiv 2\pi \ . \end{cases}$$

ii. There exists a function $\bar{\lambda}_h(\bar{\epsilon})$, $0 < \epsilon < \delta(0) \ll 1$ with

$$\bar{\lambda}_h(0) = 0, \qquad \bar{\lambda}_h(\bar{\epsilon}) = \bar{\lambda}_h(-\bar{\epsilon}) \qquad \text{and} \qquad \bar{\sigma}(\bar{\epsilon}, \bar{\lambda}_h(\bar{\epsilon})) = 0 \ .$$

iii. There exists an open neighbourhood V of the u-axis in $(u, \bar{\epsilon})$-space and two functions $\tilde{t}(u,\bar{\epsilon}) \in \mathbb{R}$ and $\tilde{\lambda}(u,\bar{\epsilon})u^2 \in \mathbb{R}$ defined in V, so that

$$\varphi(\ \cdot\ ,\ u,\ 0,\ \bar{\epsilon},\ \bar{\lambda}_h(\bar{\epsilon}) + \tilde{\lambda}(u,\bar{\epsilon})u^2), \quad u \neq 0$$

is a $\tilde{t}(u,\bar{\epsilon})$-periodic solution of the system (4.6). Additionally, one obtains

$$\tilde{t}(u,0) = T(u,E), \qquad \tilde{t}(0,\bar{\epsilon}) = 2\pi, \qquad \tilde{\lambda}(u,0) = \tfrac{3}{4}R\cdot(1 + O(Eu)),$$

$$\tilde{\lambda}(u,0) = \tilde{\lambda}(-u,0) \qquad \text{and} \qquad \tilde{\lambda}(u,0) > (<)\ 0 \qquad \text{for} \qquad R > (<)\ 0\ .$$

iv. The periodic orbits from iii are stable (unstable) for

$$\bar{\epsilon}\cdot R\cdot B > (<)\ 0, \qquad \begin{cases} 0<|u|\ll 1, & 0<|\bar{\epsilon}|\ll 1, \qquad \textit{if} \quad E\neq 0 \\ 0<|u|<\infty, & 0<|\bar{\epsilon}|<\delta(u)\ll 1, \quad \textit{if} \quad E=0\ . \end{cases}$$

Hence, under consideration of $\bar{\sigma}(0,\bar{\lambda})=0$ and ii, the surface of stationary points $(u,v,\bar{\epsilon},\bar{\lambda}) = (0,0,\bar{\epsilon},\bar{\lambda})$ (compare (4.5)) contains the two curves of Hopf points $(u,v,\bar{\epsilon},\bar{\lambda}) = (0,0,0,\bar{\lambda})$ and $(u,v,\bar{\epsilon},\bar{\lambda}) = (0,0,\bar{\epsilon},\bar{\lambda}_h(\bar{\epsilon}))$ which intersect in the central Hopf point $(u,v,\bar{\epsilon},\bar{\lambda}) = \Theta$. Then, according to i and iii, periodic orbits bifurcate from each of these curves resulting in the transversal intersection of the two manifolds of periodic orbits $(u,v,\bar{\epsilon},\bar{\lambda}) = (u,0,0,\bar{\lambda})$ and $(u,v,\bar{\epsilon},\bar{\lambda}) = (u,0,\bar{\epsilon},\bar{\lambda}_h(\bar{\epsilon}) + \tilde{\lambda}(u,\bar{\epsilon})u^2)$ along the curve of periodic bifurcation points $(u,v,\bar{\epsilon},\bar{\lambda}) = (u,0,0,\tilde{\lambda}(u,0)u^2) = (u,0,0,\frac{3}{4}\cdot Ru^2+O(Eu^3))$ with vanishing cubic u-remainder term in case of $E=0$. Summing up, for $R>0$ and $u\geq 0$, the $(\bar{\epsilon},\bar{\lambda},u)$-diagram depicted in Fig.6 below arises exemplarily in the vicinity of the bifurcation point $(u,v,\bar{\epsilon},\bar{\lambda}) = \Theta$ of the two curves of Hopf points HP.

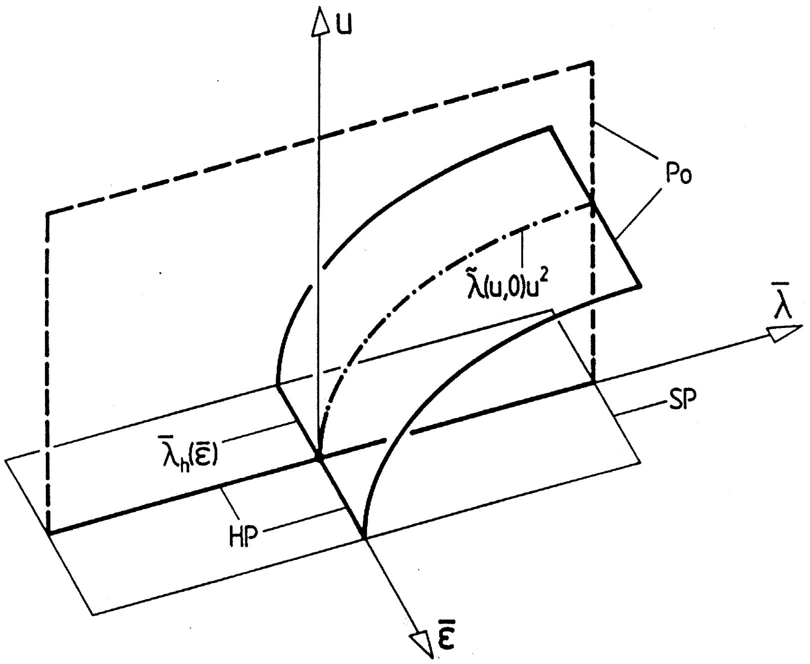

Figure 6: $(\bar{\epsilon},\bar{\lambda},u)$-bifurcation diagram near the central Hopf point. HP = Hopf point, SP = stationary point, Po = periodic orbit.

Now, in case of $E = f^0_{xx}f^0_y/d = 0$ and according to iv, the stability of the periodic orbits which bifurcate in the direction of $\bar{\epsilon}$ from $\tilde{\lambda}(u,0)u^2$ is locally determined for each $u\neq 0$, while in case of $E\neq 0$, the stability is merely determined near the central Hopf point, i.e. for $0<|u|\ll 1$. However, numerical calculations suggest (compare section 5) that also in case of $E\neq 0$ a global stability result with respect to u remains valid.

Theorem 4.1 is proved in the next section, whereas now, the back interpretation of the statements i-iv to the original system (2.1) is performed. At first, according to the complete transformation (4.7) and iii, the starting data

$$\begin{aligned}\{\epsilon,\lambda\} &= \{\epsilon,\ \epsilon\cdot[\ \bar\lambda_h(\sqrt{\epsilon})+\tilde\lambda(u,\sqrt{\epsilon})u^2-(A+G)/B\ ]\} =: \{\epsilon,\lambda^p(u,\epsilon)\},\\ x &= x^s(\epsilon,\lambda^p(u,\epsilon))+\sqrt{\epsilon}\cdot f_y^0 u = O(\sqrt{\epsilon}),\\ y &= y^s(\epsilon,\lambda^p(u,\epsilon))-\epsilon\cdot\tfrac{1}{2}f_{xx}^0 f_y^0 u^2 = O(\epsilon)\end{aligned} \tag{4.10}$$

yields a $\tilde t(u,\sqrt{\epsilon})/O(\sqrt{\epsilon})$–periodic orbit of the system (2.1) for $u,\ \epsilon>0$. Thus, for fixed $u>0$ and varying $\epsilon\geq 0$, a branch of periodic orbits starts out of the central Hopf point $(x,y,\epsilon,\lambda)=\Theta$ which possesses the properties of Theorem 2.1 ii with the notations $\lambda_h(\epsilon):=\epsilon\cdot[\bar\lambda_h(\sqrt{\epsilon})-(A+G)/B]$ and $\tau(u,\bar\epsilon):=\tilde\lambda(u,\bar\epsilon)u^2$. Moreover, for $u=0$ Theorem 4.1 ii ensures the existence of a curve of Hopf points $(x,y,\epsilon,\lambda)=(x^s(\epsilon,\lambda_h(\epsilon)),y^s(\epsilon,\lambda_h(\epsilon)),\epsilon,\lambda_h(\epsilon)) =: (x_h(\epsilon),y_h(\epsilon),\epsilon,\lambda_h(\epsilon))$ with eigenvalues of order $\pm i\cdot O(\sqrt{\epsilon})$ as ϵ tends to 0 (compare (4.5) and (4.7)). This implies the assertions of Theorem 2.1 i. Further, Theorem 4.1 iii directly yields the properties of $\tau(u,0)=\tilde\lambda(u,0)u^2$ from Theorem 2.1 iii, whereas Theorem 4.1 iv shows the stability statements of Theorem 2.1 iv.

The periodic starting data of the system (2.1) in equation (4.10) forms a 2-dimensional surface within the 4-dimensional (x,y,ϵ,λ)-space parametrized by the internal variable $\epsilon>0$ and the external variable u. Now the external u-parametrization can be replaced by an internal x-parametrization according to $(x,y,\epsilon,\lambda)=(x,y^*(x,\epsilon),\epsilon,\lambda^*(x,\epsilon))$ for (u,x) near Θ. Then, this completely internal parametrization yields the identities $\lambda_x^*(x_h(\epsilon),\epsilon)=0$ and $\lambda_{xx}^*(x_h(\epsilon),\epsilon)=2\cdot\tilde\lambda(0,\sqrt{\epsilon})/(f_y^0)^2$ along the curve of Hopf points. This leads to the indicated shape of periodic orbits Po in Fig.4 with corresponding limiting behaviour of the curvature

$$\lambda_{xx}^*(x_h(\epsilon),\epsilon)\ \rightarrow\ 2\cdot\frac{\tilde\lambda(0,0)}{(f_y^0)^2}=2\cdot\frac{3}{4}\frac{R}{(f_y^0)^2}=\frac{3}{2}\frac{R}{(f_y^0)^2}\qquad\text{as}\qquad \epsilon\ \rightarrow\ 0\ .$$

In particular, the bifurcation direction of the periodic orbits along the λ-axis is determined by the sign of $R\neq 0$, as already mentioned.

5 Proof of Theorem 4.1

The proof of Theorem 4.1 is accomplished with the help of a globally defined Poincaré-map with respect to the u-axis. For $\bar\epsilon=0$ and $u\in\mathbb{R}$ this Poincaré-map of the system (4.6) is obviously defined according to Fig.5. Further, due to the transversal intersection of the periodic orbits with the u-axis, this map can be extended in the direction of $\bar\epsilon$ for $u\neq 0$; i.e. the time of first return $\bar t(u,\bar\epsilon,\bar\lambda)$ to the positive and negative u-axis exists in an open neighbourhood of $\{(u,\bar\epsilon,\bar\lambda)|u\neq 0,\ \bar\epsilon=0\}$. Moreover, considering the eigenvalues $\bar\sigma(\bar\epsilon,\bar\lambda)\pm i$ of $H_w(\Theta,\bar\epsilon,\bar\lambda)$ (compare (4.5)) and with the notation $\bar t(0,\bar\epsilon,\bar\lambda):=2\pi$, this function of class C^∞ can be extended smoothly into the stationary points $w=(u,v)=(0,0)$. This yields a C^∞-function $\bar t(u,\bar\epsilon,\bar\lambda)$ which is defined in an open neighbourhood of $\{(u,\bar\epsilon,\bar\lambda)|\bar\epsilon=0\}$ and satisfies

$$\bar t(u,0,\bar\lambda)=T(u,E),\qquad \bar t(0,\bar\epsilon,\bar\lambda)=2\pi\qquad\text{and}\qquad \varphi_2(\bar t(u,\bar\epsilon,\bar\lambda),u,0,\bar\epsilon,\bar\lambda)=0. \tag{5.1}$$

This construction of the time of first return to the u-axis is performed in detail in [12] which goes along the lines of [1]. Furthermore, the well known relations

$$(\varphi_{1u}, \varphi_{2u})(\bar{t}, 0, 0, \bar{\epsilon}, \bar{\lambda}) = \exp(\bar{\sigma}(\bar{\epsilon}, \bar{\lambda})\bar{t}) \cdot (\cos(\bar{t}), -\sin(\bar{t})) \tag{5.2}$$

are valid in the stationary points. Now, the periodic orbits can be interpreted as solutions of the equation

$$\varphi_1(\bar{t}(u, \bar{\epsilon}, \bar{\lambda}), u, 0, \bar{\epsilon}, \bar{\lambda}) - u =: V(u, \bar{\epsilon}, \bar{\lambda}) = 0$$

which possesses the trivial zeros $V(u, 0, \bar{\lambda}) = 0$ and $V(0, \bar{\epsilon}, \bar{\lambda}) = 0$ (compare the integral system (4.8) and the stationary points). Thus, a Taylor expansion with respect to $\bar{\epsilon}$ yields

$$V(u, \bar{\epsilon}, \bar{\lambda}) = \bar{\epsilon} \cdot \{\varphi_{1\bar{\epsilon}}(T(u, E), u, 0, 0, \bar{\lambda}) + O(\bar{\epsilon})\} =: \bar{\epsilon} \cdot V_1(u, \bar{\epsilon}, \bar{\lambda}) \tag{5.3}$$

where $\varphi_{\bar{\epsilon}}(\bar{t}, u, 0, 0, \bar{\lambda})$ satisfies $\varphi_{\bar{\epsilon}}(0, u, 0, 0, \bar{\lambda}) = \Theta$ and

$$\dot{\varphi}_{\bar{\epsilon}}(\bar{t}, u, 0, 0, \bar{\lambda}) = H_w(\phi(\bar{t}, u, 0, E), 0, \bar{\lambda}) \cdot \varphi_{\bar{\epsilon}}(\bar{t}, u, 0, 0, \bar{\lambda}) + H_{\bar{\epsilon}}(\phi(\bar{t}, u, 0, E), 0, \bar{\lambda}). \tag{5.4}$$

Then, with $U(\bar{t}, u) = (\phi_u, \phi_v)(\bar{t}, u, 0, E)$ and $U_i(\bar{t}, u)$ as well as $U_i(\bar{t}, u)^{-1}$ denoting the fundamental matrix of the homogenous part $\dot{w} = H_w(\phi(\bar{t}, u, 0, E), 0, \bar{\lambda})w$ and the i-th row of $U(\bar{t}, u)$ and $U(\bar{t}, u)^{-1}$ respectively, the subsequent identities follow after a simple calculation with the help of the adjoint equation $\dot{w} = -H_w^t(\phi(\bar{t}, u, 0, E), 0, \bar{\lambda})w$

$$U_1(T(u, E), u) = (1, 0) \qquad \text{and} \qquad U_1(\bar{t}, u)^{-1} = \frac{1}{u} \cdot \left(\phi_1 \ , \ \frac{-\phi_2}{E\phi_2 - 1}\right)(\bar{t}, u, 0, E), \qquad u \neq 0 \ .$$

Hence, equation (5.4) and the variation of constants formula yield

$$\varphi_{1\bar{\epsilon}}(T(u, E), u, 0, 0, \bar{\lambda}) = \int_0^{T(u,E)} \frac{1}{u} \cdot \left(\phi_1 \ , \ \frac{-\phi_2}{E\phi_2 - 1}\right)(s, u, 0, E) \cdot H_{\bar{\epsilon}}(\phi(s, u, 0, E), 0, \bar{\lambda}) \ ds \ .$$

For $u \neq 0$ this implies the following equivalence (cf. (4.6), (4.8), (5.3) and some partial integrations)

$$V_1(u, 0, \bar{\lambda}) = -\frac{1}{u} \int_0^{T(u,E)} \frac{1}{E\phi_2(s, u, 0, E) - 1} \cdot \left(B\bar{\lambda}\phi_1^2 + \frac{(C + F)E + 3D}{3} \ \phi_1^4\right)(s, u, 0, E) \ ds = 0$$

$$\Leftrightarrow \quad \bar{\lambda} \quad = \quad \frac{(C + F)E + 3D}{-3B} \cdot \frac{\displaystyle\int_0^{T(u,E)} \frac{\phi_1^4(s, u, 0, E)}{E\phi_2(s, u, 0, E) - 1} \ ds}{\displaystyle\int_0^{T(u,E)} \frac{\phi_1^2(s, u, 0, E)}{E\phi_2(s, u, 0, E) - 1} \ ds} \quad =: \quad R \cdot S(u, E) \tag{5.5}$$

where the C^∞-function $S(\cdot, \cdot)$ satisfies

$$S(u, E) > 0 \qquad \text{and} \qquad S(u, E) = S(-u, E). \tag{5.6}$$

Now, because of $V_{1\bar{\lambda}}(u, 0, RS(u, E)) \neq 0$ (compare $B \neq 0$ and (5.5)), the solutions $V_1(u, 0, RS(u, E)) = 0$, $u \neq 0$ can be uniquely continued in the direction of $\bar{\epsilon}$ implying the existence of a unique C^∞-function $\bar{\lambda}(u, \bar{\epsilon})$ with

$$\bar{\lambda}(u, 0) = R \cdot S(u, E) \qquad \text{and} \qquad V_1(u, \bar{\epsilon}, \bar{\lambda}(u, \bar{\epsilon})) = 0 \tag{5.7}$$

defined in an open neighbourhood of the punctured u-axis $\{u \in \mathbb{R}\}/\{0\}$. Moreover, in view of $\varphi(\bar{t},0,0,\bar{\epsilon},\bar{\lambda}) = \Theta$, $\bar{\sigma}(\bar{\epsilon},\bar{\lambda}) = \frac{1}{2}\cdot \mathrm{tr}(H_w)(\Theta,\bar{\epsilon},\bar{\lambda})$ and (4.6), (5.2),(5.3), a Taylor expansion with respect to u of $V_1(u,\bar{\epsilon},\bar{\lambda})$ results in the identities

$$\begin{aligned} V(u,\bar{\epsilon},\bar{\lambda}) &= \bar{\epsilon}\cdot u\cdot \{\varphi_{1\bar{\epsilon}u}(2\pi,0,0,0,\bar{\lambda}) + O(u) + O(\bar{\epsilon})\} \\ &= \bar{\epsilon}\cdot u\cdot \{2\pi\cdot \bar{\sigma}_{\bar{\epsilon}}(0,\bar{\lambda}) + O(u) + O(\bar{\epsilon})\} \\ &= \bar{\epsilon}\cdot u\cdot \{\pi\cdot B\bar{\lambda} + O(u) + O(\bar{\epsilon})\} =: \bar{\epsilon}\cdot u\cdot V_2(u,\bar{\epsilon},\bar{\lambda}) \end{aligned}$$

yielding the unique solution $\bar{\lambda} = 0$ of $V_2(0,0,\bar{\lambda}) = 0$. Due to $V_{2\bar{\lambda}}(0,0,0) = \pi\cdot B \neq 0$ this solution can be uniquely continued in the direction of $\bar{\epsilon}$. Therefore, the functions $S(u,E)$ and $\bar{\lambda}(u,\bar{\epsilon})$ from equation (5.7) can be extended smoothly to $u = 0$ that means onto the complete u-axis and an open neighbourhood of this axis respectively. Summing up, for $u \neq 0$ the points $(u,v,\bar{\epsilon},\bar{\lambda}) = (u,0,\bar{\epsilon},\bar{\lambda}(u,\bar{\epsilon}))$ represent a 2-dimensional surface of periodic starting data of the system (4.6) ensuring the pure existence of the nontrivial manifold of periodic orbits claimed in Fig.6. Moreover, a simple calculation shows that the intersection of this manifold with the manifold of stationary points $(u,v,\bar{\epsilon},\bar{\lambda}) = (0,0,\bar{\epsilon},\bar{\lambda})$ forms a curve of Hopf points $(u,v,\bar{\epsilon},\bar{\lambda}) = (0,0,\bar{\epsilon},\bar{\lambda}(0,\bar{\epsilon})) =: (0,0,\bar{\epsilon},\bar{\lambda}_h(\bar{\epsilon}))$ for $u = 0$ with

$$\bar{\lambda}_h(0) = 0 \qquad \text{and} \qquad \bar{\lambda}_h(\bar{\epsilon}) = \bar{\lambda}_h(-\bar{\epsilon}) \tag{5.8}$$

(compare (4.5)). Furthermore, in these Hopf points the relations

$$\bar{\lambda}_u(0,\bar{\epsilon}) = 0, \qquad \bar{\lambda}_{uu}(0,\bar{\epsilon}) = -\frac{1}{3}\frac{V_{uuu}(0,\bar{\epsilon},\bar{\lambda}_h(\bar{\epsilon}))}{V_{u\bar{\lambda}}(0,\bar{\epsilon},\bar{\lambda}_h(\bar{\epsilon}))} \qquad \text{for} \qquad \bar{\epsilon} \neq 0 \tag{5.9}$$

with

$$\begin{aligned} V_{uuu}(0,\bar{\epsilon},\bar{\lambda}_h(\bar{\epsilon})) \;&=\; \frac{3\pi}{4}\cdot (H_{1uuu} + H_{1uvv} + H_{2uuv} + H_{2vvv} - H_{1uv}(H_{1uu} + H_{1vv}) \\ &\quad + H_{2uv}(H_{2uu} + H_{2vv}) + H_{1uu}H_{2uu} - H_{1vv}H_{2vv})(\Theta,\bar{\epsilon},\bar{\lambda}_h(\bar{\epsilon})) \\ &= \frac{3\pi}{2}\cdot \bar{\epsilon}\cdot ((C+F)E + 3D) + O(\bar{\epsilon}^2) = -\frac{9\pi}{2}\cdot \bar{\epsilon}\cdot R\cdot B + O(\bar{\epsilon}^2) \end{aligned}$$

and

$$V_{u\bar{\lambda}}(0,\bar{\epsilon},\bar{\lambda}_h(\bar{\epsilon})) = \bar{\epsilon}\cdot \pi\cdot B + O(\bar{\epsilon}^2)$$

hold true (compare for example [11]). This implies $\bar{\lambda}_{uu}(0,0) = 3R/2$ and

$$\bar{\lambda}(u,\bar{\epsilon}) = \bar{\lambda}(0,\bar{\epsilon}) + (\tfrac{1}{2}\bar{\lambda}_{uu}(0,\bar{\epsilon}) + O(u))\cdot u^2 =: \bar{\lambda}_h(\bar{\epsilon}) + \tilde{\lambda}(u,\bar{\epsilon})\cdot u^2 \ . \tag{5.10}$$

In particular, for $\bar{\epsilon} = 0$ one obtains according to (5.7)

$$\bar{\lambda}(u,0) = \tilde{\lambda}(u,0)\cdot u^2 = (\tfrac{3}{4}R + O(u))\cdot u^2 = R\cdot S(u,E)$$

yielding $S(0,E) = S_u(0,E) \equiv 0$ and $S_{uu}(0,E) \equiv \frac{3}{2}$. Further, an explicit calculation performed with $E = 0$ shows $S(u,0) = \frac{3}{4}u^2$ (compare (4.9), (5.5)) and an examination of the Taylor expansion of $S(u,E)$ implies $S(u,E) = \frac{3}{4}u^2 + O(Eu^3)$. This proves Theorem

4.1 i–iii under consideration of Fig.5, the equations (4.9), (5.1), (5.6)–(5.8) and the setting $\tilde{t}(u,\bar{\epsilon}) := \bar{t}(u,\bar{\epsilon},\bar{\lambda}(u,\bar{\epsilon}))$.

In the last step, the stability properties in Theorem 4.1 iv of the periodic solutions $\varphi(\bar{t},u,0,\bar{\epsilon},\bar{\lambda}(u,\bar{\epsilon}))$, $u \neq 0$ are derived with the help of the equation

$$Q(u,\bar{\epsilon},\bar{\lambda}) := \int_0^{\bar{t}(u,\bar{\epsilon},\bar{\lambda})} \mathrm{tr}(H_w)(\varphi(s,u,0,\bar{\epsilon},\bar{\lambda}),\bar{\epsilon},\bar{\lambda})\ ds \tag{5.11}$$

$$= \int_0^{\bar{t}(u,\bar{\epsilon},\bar{\lambda})} E\varphi_1(\cdot) + \bar{\epsilon}\cdot(B\bar{\lambda} + (-\tfrac{1}{2}BE\bar{\lambda} + C + GE)\varphi_2 + (3D+CE)\varphi_1^2)(\cdot) + O(\bar{\epsilon}^2)\ ds \ = \ 0$$

(compare (4.6)). Note that the product of the Floquet multipliers of a periodic orbit reads $\exp[Q(u,\bar{\epsilon},\bar{\lambda}(u,\bar{\epsilon}))]$. Now, if it is possible to show for $R > 0$ and without loss of generality for $u \geq 0$ the structures within Fig.7 below, then the stability conditions on the manifold of periodic orbits $\bar{\lambda}(u,\bar{\epsilon}) = \bar{\lambda}_h(\bar{\epsilon}) + \tilde{\lambda}(u,\bar{\epsilon})u_1^2$, $u\bar{\epsilon} \neq 0$ follow directly from the sign of Q above the surface $Q = 0$. Of course, an analogous statement is valid for $R < 0$.

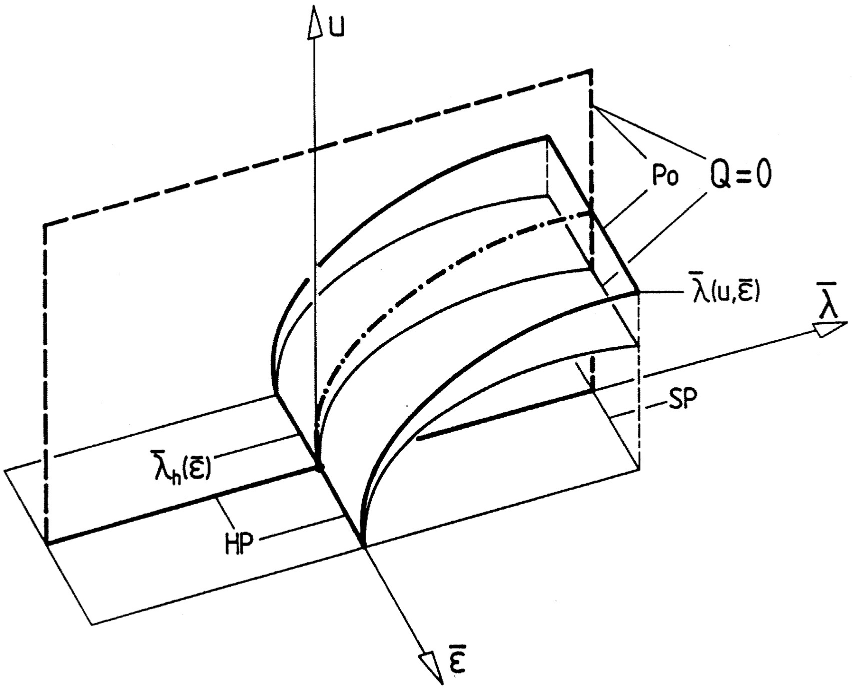

Figure 7: The stability of the periodic orbits is determined by the sign of Q. HP = Hopf point, SP = stationary point, Po = periodic orbit.

First of all, the equation $Q = 0$ obviously possesses for $\bar{\epsilon} = 0$ the trivial zeros $Q(u,0,\bar{\lambda}) = 0$ (compare Fig.5) and thus an expansion of Q with respect to $\bar{\epsilon}$ yields

$$Q(u,\bar{\epsilon},\bar{\lambda}) = \bar{\epsilon}\cdot(Q_{\bar{\epsilon}}(u,0,\bar{\lambda}) + O(\bar{\epsilon})) =: \bar{\epsilon}\cdot Q_1(u,\bar{\epsilon},\bar{\lambda})$$

implying for $\bar{\epsilon} = 0$ with $(\cdot) = (s, u, 0, 0, \bar{\lambda})$ and $\varphi(\bar{t}, 0, 0, \bar{\epsilon}, \bar{\lambda}) = \Theta$ the relations

$$Q_1(u, 0, \bar{\lambda}) = \int_0^{T(u,E)} E\varphi_{1\bar{\epsilon}}(\cdot) + (3D + CE)\varphi_1^2(\cdot)\ ds + T(u, E)\cdot B\bar{\lambda} + \bar{t}_{\bar{\epsilon}}(u, 0, \bar{\lambda})\cdot Eu,$$

$$Q_1(0, 0, \bar{\lambda}) = Q_{\bar{\epsilon}}(0, 0, \bar{\lambda}) = T(0, E)\cdot B\bar{\lambda} = 2\pi\cdot B\bar{\lambda}\ . \tag{5.12}$$

Then, the inequality $B \neq 0$ ensures the existence of a unique function $\hat{\lambda}(u, \bar{\epsilon})$ of class C^∞ with $\hat{\lambda}(0, 0) = 0$ and $Q_1(u, \bar{\epsilon}, \hat{\lambda}(u, \bar{\epsilon})) = 0$, so that the zeros of $Q = \bar{\epsilon}\cdot Q_1$ are exactly determined by $(u, \bar{\epsilon}, \bar{\lambda}) = (u, 0, \bar{\lambda})$ and $(u, \bar{\epsilon}, \bar{\lambda}) = (u, \bar{\epsilon}, \hat{\lambda}(u, \bar{\epsilon}))$ in a neighbourhood of the central Hopf point. Moreover, according to (5.11), the identities $Q(0, \bar{\epsilon}, \bar{\lambda}_h(\bar{\epsilon})) = 2\pi\cdot \mathrm{tr}(H_w)(\Theta, \bar{\epsilon}, \bar{\lambda}_h(\bar{\epsilon})) = 0$ are valid along the curve of Hopf points $(u, v, \bar{\epsilon}, \bar{\lambda}) = (0, 0, \bar{\epsilon}, \bar{\lambda}_h(\bar{\epsilon}))$ implying $\hat{\lambda}(0, \bar{\epsilon}) = \bar{\lambda}_h(\bar{\epsilon}) = \bar{\lambda}(0, \bar{\epsilon})$, as a consequence of uniqueness. Hence, under consideration of $\bar{\lambda}_u(0, \bar{\epsilon}) = 0$ (compare (5.9)), it remains to show

$$\hat{\lambda}_u(0, \bar{\epsilon}) = 0 \qquad \text{and} \qquad \hat{\lambda}_{uu}(0, \bar{\epsilon}) > (<)\ \bar{\lambda}_{uu}(0, \bar{\epsilon}) \qquad \text{if} \qquad R > (<)\ 0 \tag{5.13}$$

for proving the correctness of Fig.7. Now, differentiation of $Q(u, \bar{\epsilon}, \hat{\lambda}(u, \bar{\epsilon})) = 0$ with respect to u yields for $u = 0$

$$Q_u(0, \bar{\epsilon}, \hat{\lambda}(0, \bar{\epsilon})) + Q_{\bar{\lambda}}(0, \bar{\epsilon}, \hat{\lambda}(0, \bar{\epsilon}))\cdot \hat{\lambda}_u(0, \bar{\epsilon}) = 0$$

with $Q_{\bar{\lambda}}(0, \bar{\epsilon}, \hat{\lambda}(0, \bar{\epsilon})) = \bar{\epsilon}\cdot Q_{1\bar{\lambda}}(0, \bar{\epsilon}, \hat{\lambda}(0, \bar{\epsilon})) \neq 0$ for $\bar{\epsilon} \neq 0$ (compare (5.12)) and $Q_u(0, \bar{\epsilon}, \hat{\lambda}(0, \bar{\epsilon})) = 0$ as the result of a simple calculation performed under consideration of (5.2) and (5.11). Therefore, the first assertion in (5.13) is shown. Correspondingly, twofold differentiation of $Q_1(u, 0, \hat{\lambda}(u, 0)) = 0$ implies $Q_{1uu}(\Theta) + 2\pi B\cdot \hat{\lambda}_{uu}(\Theta) = 0$, so that the precise determination of $\hat{\lambda}_{uu}(\Theta)$ depends on $Q_{1uu}(\Theta)$ which can be investigated again with the help of equation (5.12). However, concerning these technical calculations it is refered to [12] finally resulting in $Q_{1uu}(\Theta) = -6\pi\cdot RB$ which implies $\hat{\lambda}_{uu}(\Theta) = 3R = 2\bar{\lambda}_{uu}(\Theta)$ and the claimed inequalities in (5.13).

Further, for $\bar{\epsilon} \neq 0$ the sign of Q on the left and right side of the surface defined by $Q = \bar{\epsilon}\cdot Q_1 = 0$ (compare Fig.7) is locally fixed by the sign of $Q_{1\bar{\lambda}}(\Theta) = 2\pi\cdot B \neq 0$ (compare (5.12)), so that the stability of the periodic orbits is determined by the sign of the product $\bar{\epsilon}\cdot R\cdot B \neq 0$, as asserted in Theorem 4.1 iv. Moreover, for $E = 0$ the equations (2.6), (5.7), (5.12) together with the identities $T(u, 0) = 2\pi$, $\varphi_1(s, u, 0, 0, \bar{\lambda}) = \phi_1(s, u, 0, 0) = u\cdot\cos(s)$ (compare (4.9)) yield the relations

$$\begin{aligned} Q_1(u, 0, \bar{\lambda}(u, 0)) &= BR\cdot[\ T(u, 0)\cdot S(u, 0)\ -\ 3\int_0^{T(u,0)} \phi_1^2(s, u, 0, 0)\ ds\ ] =: BR\cdot \bar{Q}(u, 0) \\ &= BR\cdot[\ -\tfrac{3}{2}\pi u^2\ ] \neq 0 \qquad \text{for} \qquad BR\cdot u \neq 0 \end{aligned}$$

implying finally the global stability properties of the periodic orbits claimed in Theorem 4.1 iv for $E = 0$. In addition, it should be noted that also in case of $E \neq 0$, the representation

$$Q_1(u, 0, \bar{\lambda}(u, 0)) = BR\cdot[\ T(u, E)\cdot S(u, E)\ -\ 3\int_0^{T(u,E)} \phi_1^2(s, u, 0, E)\ ds\ ] =: BR\cdot \bar{Q}(u, E)$$

is valid. However the solution $\phi(s,u,0,E)$ is not known explicitly which complicates the global discussion of $\bar{Q}(u,E)$. Yet, a direct calculation shows $S(u,E) = S(Eu,1)/E^2$ and $\bar{Q}(u,E) = \bar{Q}(Eu,1)/E^2$ leading to the investigation of $S(u,1)$ and $\bar{Q}(u,1)$. Now, a numerical evaluation of these functions shows the following properties.

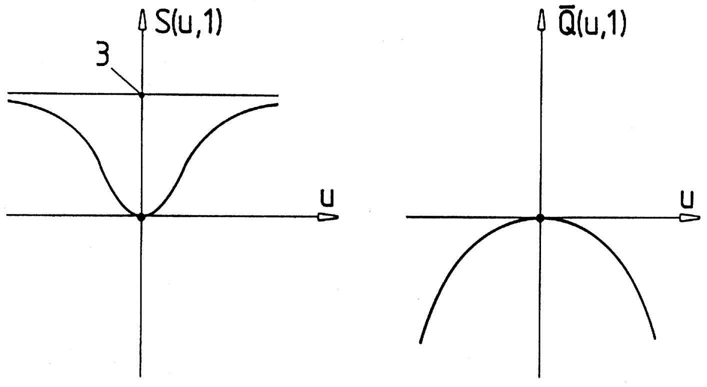

Figure 8: Numerically calculated global behaviour of $S(u,1)$ and $\bar{Q}(u,1)$ for $E=1$.

Thus, according to the numerical calculations, the function $S(u,1)$ converges strictly monotone to the value 3 as u tends to $\pm\infty$ implying the strictly monotone convergence of $\tau(u,0) = R\cdot S(u,E) = R\cdot S(Eu,1)/E^2$ towards $3R/E^2$. In particular, the claimed properties concerning the border $\hat{\lambda}(\epsilon)$ of the hatched sector in Fig.3 are shown at least numerically. Finally, the function $\bar{Q}(u,1)$ does not possess a zero for $u \neq 0$ suggesting the global stability with respect to u not only for $E=0$ (compare Theorem 4.1 iv) but also for $E \neq 0$.

Acknowledgement: This paper is part of the authors thesis written under the supervision of Prof. E. Bohl at the University of Konstanz. The final form was carried out during a four-month visit at the University of Bielefeld. The author wishes to express his thanks to Prof. E. Bohl and Prof. W.-J. Beyn.

References

[1] Andronov A. A., Leontovich E. A., Gordon I. I., Maier A. G. (1973): Theory of Bifurcations of Dynamic Systems on a Plane. Wiley

[2] Arnold V. I., Afrajmovich V. S., Il'yashenko Y. S., Shil'nikov L. P. (1994): Dynamical Systems V: Bifurcation Theory. Springer, Berlin, New York.

[3] Baer S. M., Erneux T. (1986): Singular hopf bifurcation to relaxation oscillations. SIAM J. Appl. Math. **46**, 5, 721–739.

[4] Baer S. M., Erneux T. (1992): Singular hopf bifurcation to relaxation oscillations II. SIAM J. Appl. Math. **52**, 6, 1651–1664.

[5] Diener M. (1981): Étude générique des canards. IRMA, Strasbourg.

[6] Eckhaus W. (1983): Relaxation oscillations including a standard chase on french ducks. In: Lecture notes in Mathematics 985, 449-494, Springer, Berlin, New York.

[7] Fenichel N. (1979): Geometric singular perturbation theory for ordinary differential equations. J. Differential Equations **31**, 53–98.

[8] Guckenheimer J., Holmes P. J. (1983): Nonlinear Oscillations, Dynamical Systems, and Bifurcations of Vector Fields. Springer, Berlin, New York.

[9] Koper M. (1995): Bifurcations of mixed-mode oscillations in a three-variable autonomous Van der Pol-Duffing model with a cross-shaped phase diagram. Physica **D80**, 72–94.

[10] Kuznetsov Y. A. (1995): Elements of Applied Bifurcation Theory. Appl. Math. Sci. **112**, Springer, Berlin, New York.

[11] Marsden J. E., McCracken M. (1976): The Hopf Bifurcation and Its Applications. Appl. Math. Sci. **19**, Springer, Berlin, New York.

[12] Stiefenhofer M. (1995): Singuläre Störung und Verzweigung bei Schleimpilzen. Dissertation, Hartung-Gorre, Konstanz.

[13] Vasil'eva A. B. (1963): Asymptotic behaviour of solutions to certain problems involving nonlinear differential equations containing a small parameter multiplying the highest derivatives. Russian Math. Surveys **18**, 13–84.